

A new method to study the EMC Effect using the F_2^n structure function

H. Szumila-Vance¹, I. Cloet², C. Keppel¹, S. Escalante³, N. Kalantarians³

¹Thomas Jefferson National Accelerator Facility, Newport News, VA

²Argonne National Laboratory, Argonne, IL

³Virginia Union University, Richmond, VA

Abstract

The persistently mysterious deviations from unity of the ratio of nuclear target structure functions to those of deuterium as measured in deep inelastic scattering (termed the “EMC Effect”) have become the canonical observable for studies of nuclear medium modifications to free nucleon structure in the valence regime. The structure function of the free proton is well known from numerous experiments spanning decades. The free neutron structure function, however, has remained difficult to access. Only recently has it been extracted in a systematic study of the global data within a parton distribution function extraction framework and is available from the CTEQ-Jefferson Lab (CJ) Collaboration. Here we leverage the latter to introduce a new method to study the EMC Effect in nuclei by re-examining existing data and by now determining the magnitude of the medium modifications to the free neutron and proton structure functions independently. From the extraction of the free neutron from world data, it is possible to examine the nuclear effects in deuterium and their contribution to our interpretation of the EMC Effect. In this study, we observe that the ratio of the deuteron to the sum of the free neutron and proton structure functions has some x_B and Q^2 dependencies implying that the magnitude of the standard EMC Effect is in part due to the nuclear effects of the deuteron and also exhibits some x_B and Q^2 dependence.

1 Introduction

The EMC Effect

We chose to use the SLAC E139 data set because it is the most complete published list of cross sections available. From the initial cross sections given, we converted the absolute cross section to the structure function by using the kinematics and R1990 fitting.

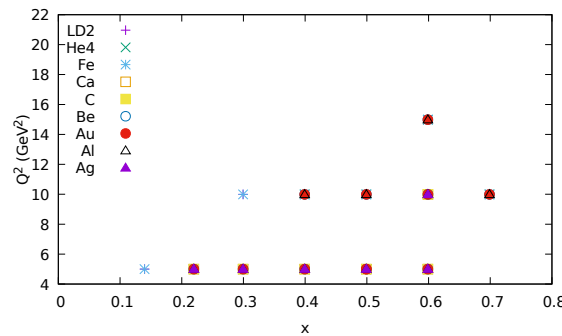


Figure 1

2 Theory predictions using nuclear matter

Discussion points: predicted d/n and d/p ratios, interpretations in quark distributions, emc effects in deuterium

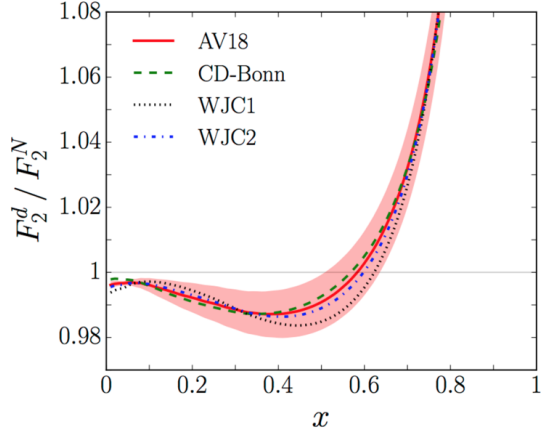


Figure 2: The theoretical extraction of the ratio of F_2^d / F_2^N . The deuteron exhibits some x_B -dependence such that the ratio is modified by approximately 2% in the regime of x_B between 0.3–0.7 (region of interest to the EMC Effect).

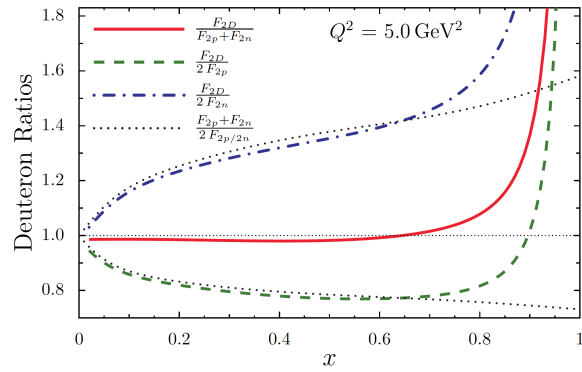


Figure 3: Theoretically-derived deuteron F_2 ratios with respect to the free neutron and proton, the free proton, and the free neutron are shown for $Q^2 = 5$.

3 F_2^n extraction and the CJ15 fit

We need to point to CJ and how the world data was extracted.

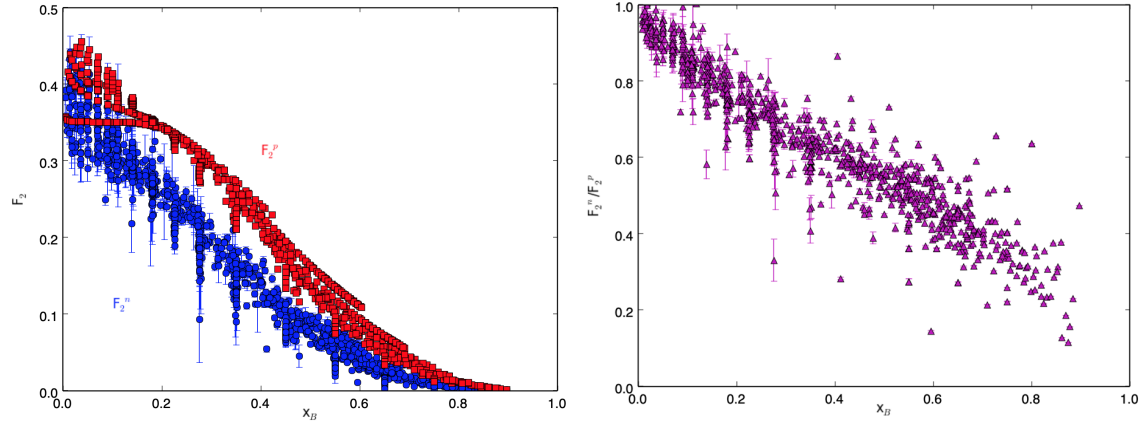


Figure 4: Left: The extracted F_2^n from the world DIS data is shown in blue, and the F_2^p from the NMC global fit is shown in red for the same corresponding x_B and Q^2 . Right: The ratio of the F_2^n / F_2^p from the left is shown as a function of x_B .

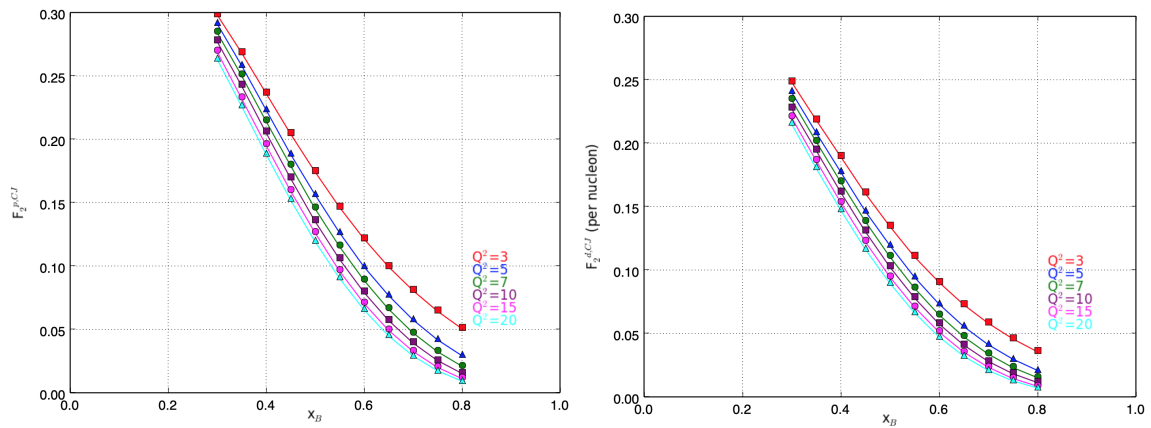


Figure 5: Left: The proton structure function from the CJ15 fit is shown as a function of x_B for various fixed Q^2 . Right: The deuteron structure function from the CJ15 fit is shown as a function of x_B for various fixed Q^2 .

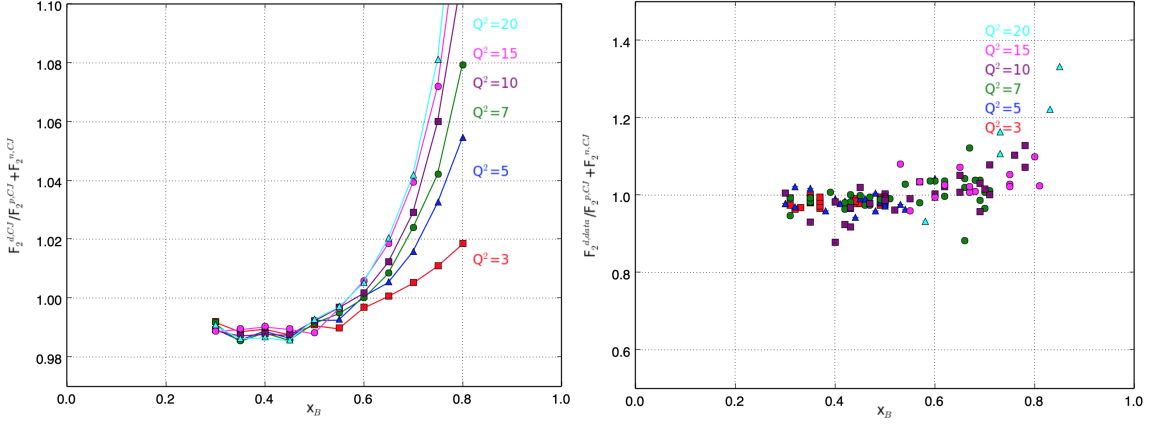


Figure 6: Left: The deuteron structure function divided by the sum of the free proton and free neutron structure functions from the CJ15 fit is shown for various Q^2 . This ratio roughly shows the magnitude of the nuclear effects in the deuteron. The Q^2 dependence shows significant spread above $x_B = 0.6$ where the ratio begins to increase. Right: The global Whitlow deuterium data from SLAC [7] is shown divided by the sum of the free proton and free neutron structure functions from the CJ15 fit.

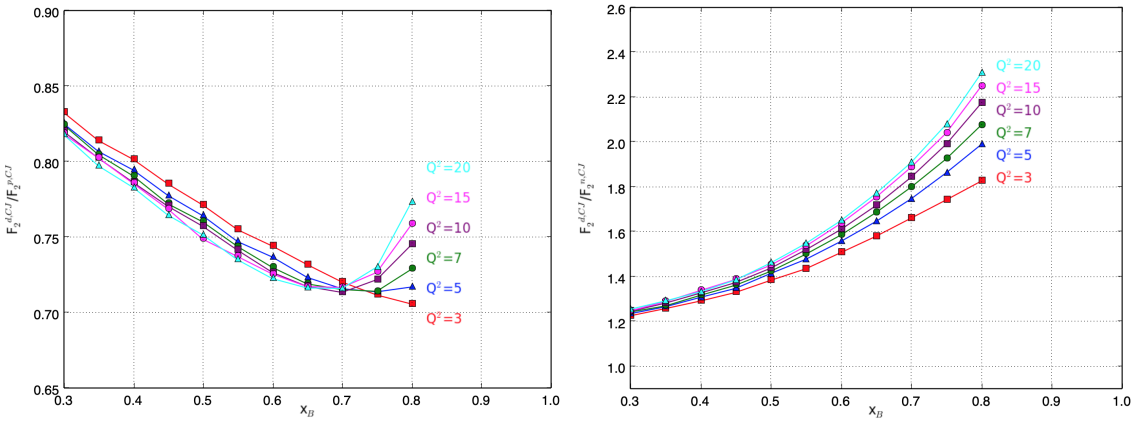


Figure 7: Left: The deuterium structure function from the CJ15 fit is shown as a ratio to the proton structure function from CJ15 for various Q^2 . Right: The deuterium structure function from the CJ15 fit is shown as a ratio to the neutron structure function from CJ15 for various Q^2 .

3.1. Q^2 dependence

4 Structure function extraction from the E139 cross sections

Most experiments officially publish the extracted F_2 ratios. For this analysis, the experimental cross sections were desirable for the flexibility to construct and study the F_2 ratios for the nucleus of interest relative to various free nucleon quantities. The SLAC E139 experiment published the experimental cross sections for the following nuclei: deuterium, helium, beryllium, carbon, aluminum, calcium, iron, silver and gold. The cross sections include published statistical and systematic errors. The F_2 structure function for each nucleus is extracted from the cross section using the relationship shown in Equation (1).

$$F_2 = \frac{d^2\sigma}{d\Omega dE'} \frac{1+R}{1+\epsilon R} \frac{K\nu}{4\pi^2\alpha\Gamma(1+\nu^2/Q^2)} \quad (1)$$

From Equation (1), ϵ , K , and Γ are defined by the usual quantities of the electron scattering kinematics in Equation (4). These quantities include the measured scattering angle θ , the momentum transfer Q^2 , the energy transfer ν , the scattered electron energy E' , the mass of the proton M , and the squared invariant mass W^2 .

$$\epsilon = (1 + 2 \frac{\nu^2 + Q^2}{Q^2} \tan^2 \frac{\theta}{2})^{-1} \quad (2)$$

$$K = \frac{W^2 - M^2}{2M} \quad (3)$$

$$\Gamma = \frac{\alpha KE'}{2\pi^2 Q^2 E(1-\epsilon)} \quad (4)$$

For most published cross section ratios, corrections are applied to account for the excess of neutrons in asymmetric nuclei. This correction is referred to as the "isoscalar correction" and is defined in Equation (5). While this correction is not applied in this paper for the F_2 ratios per free proton and free neutron, it is relevant for accurately reconstructing the published F_2^A/F_2^d cross sections as in most analyses.

$$f_{iso}^A = \frac{\frac{1}{2}(1 + F_2^n/F_2^p)}{\frac{1}{A}(Z + (A-Z)F_2^n/F_2^p)} \quad (5)$$

From the analysis described in this section, the carbon and gold F_2^A/F_2^d ratios are reconstructed (with the iso-scalar correction applied to gold) and compared to the published ratios in the EMC and NMC experiments as shown in Fig. 8.

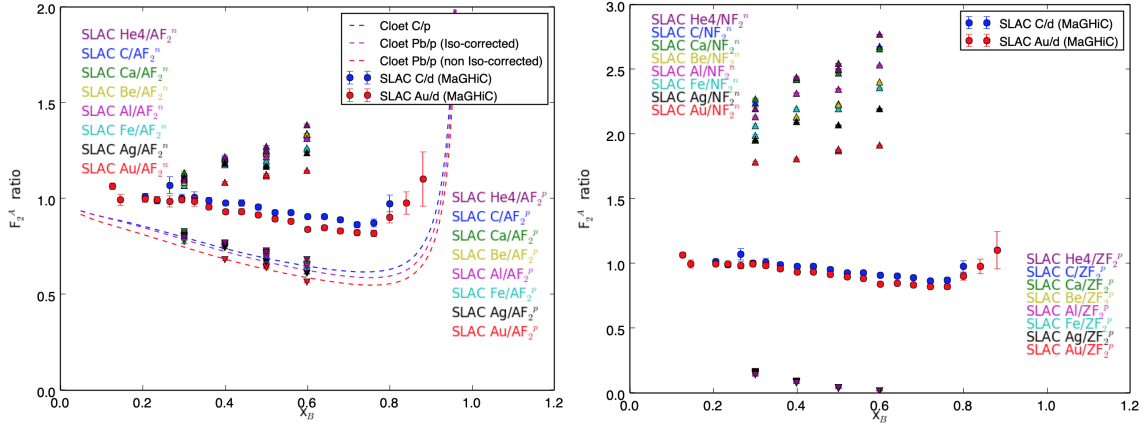


Figure 9: Left: F_2^A calculated from the published SLAC E139 cross sections is taken as a ratio per nucleon to F_2^n and F_2^p , separately. The published EMC ratios for carbon and gold [9] are shown for reference as F_2^A/F_2^d per nucleon. Theory predictions for the F_2^A structure function per nucleon as a ratio to F_2^p are shown. Right: F_2^A calculated from the published SLAC E139 cross sections is taken as a ratio per neutron or proton and F_2^n and F_2^p , separately. The published EMC ratios for carbon and gold [9] are shown for reference.

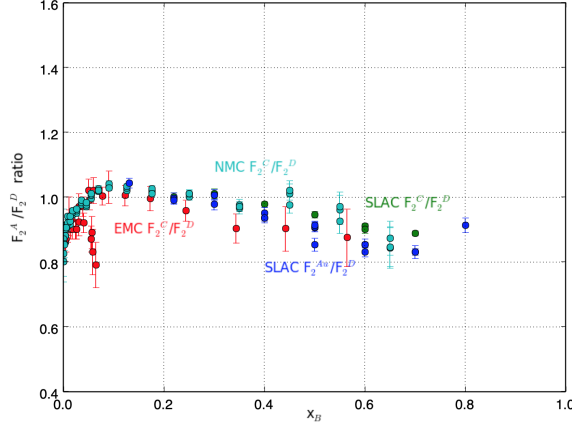


Figure 8: The published structure function ratios per nucleon for carbon and gold are shown from SLAC, NMC, and the EMC experiments.

The carbon ratio from the SLAC E139 experiment is consistent with the ratio found in the EMC and NMC experiments, and the carbon exhibits a shallower slope with respect to x_B as compared to the heavier, iso-scalar corrected gold ratio.

5 General observations

6 Deuterium nuclear effects and heavier nuclei

6.1. Deuterium

plots: include d/n or n/d of Whitlow+BONUS to show Q2 dependency

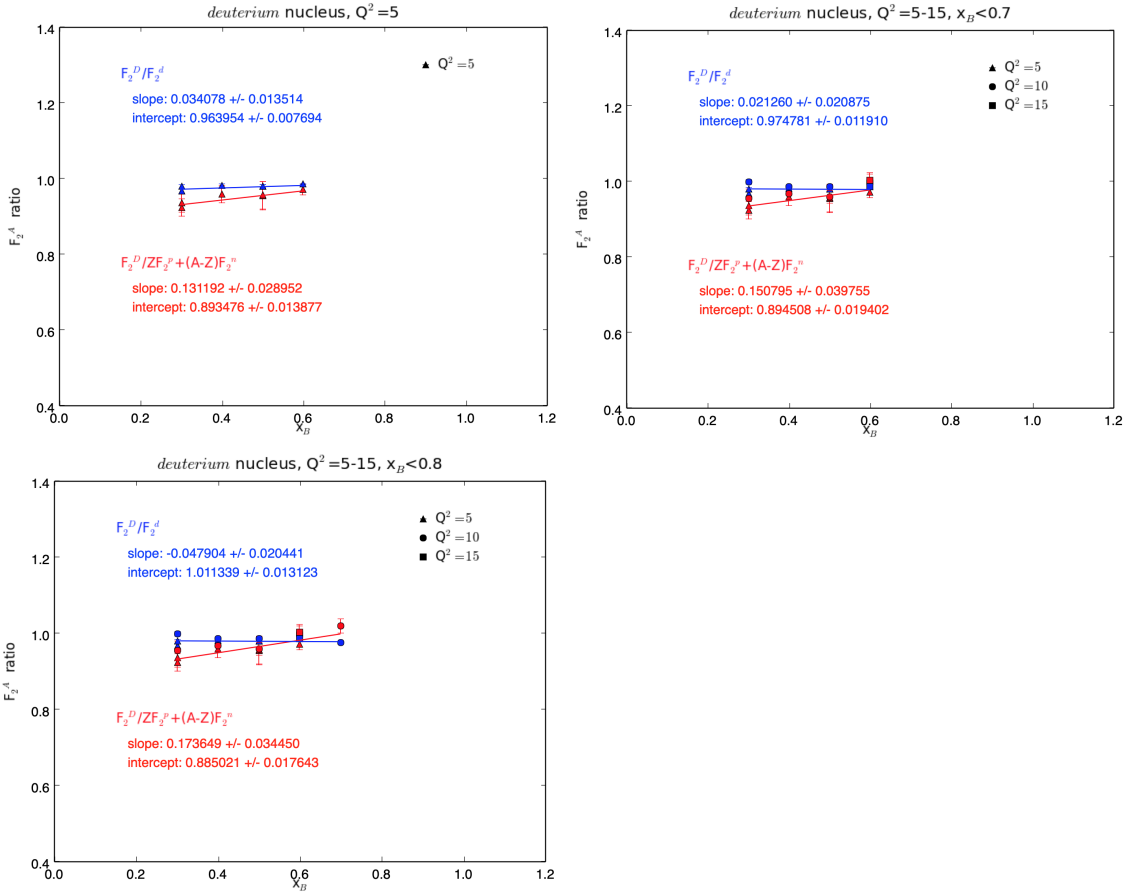


Figure 10: Linear fits to the deuterium target data with cuts on Q^2 and x_B .

6.2. Heavier nuclei

7 Conclusions

8 Acknowledgments

The authors would like to thank Shujie Li for constructing the most complete world F_2^n data set to date and Alberto Accardi and Wally Melnitchouk for providing crucial insights and interpretations for this analysis.

References

- [1] A. Accardi, L. T. Brady, W. Melnitchouk, J. F. Owens and N. Sato, Phys.Rev. D93 (2016) 114017
- [2] J. Gomez *et al.*, “Measurement of the A-dependence of deep inelastic electron scattering,” Phys. Rev. D **49**, 4348 (1994). doi:10.1103/PhysRevD.49.4348

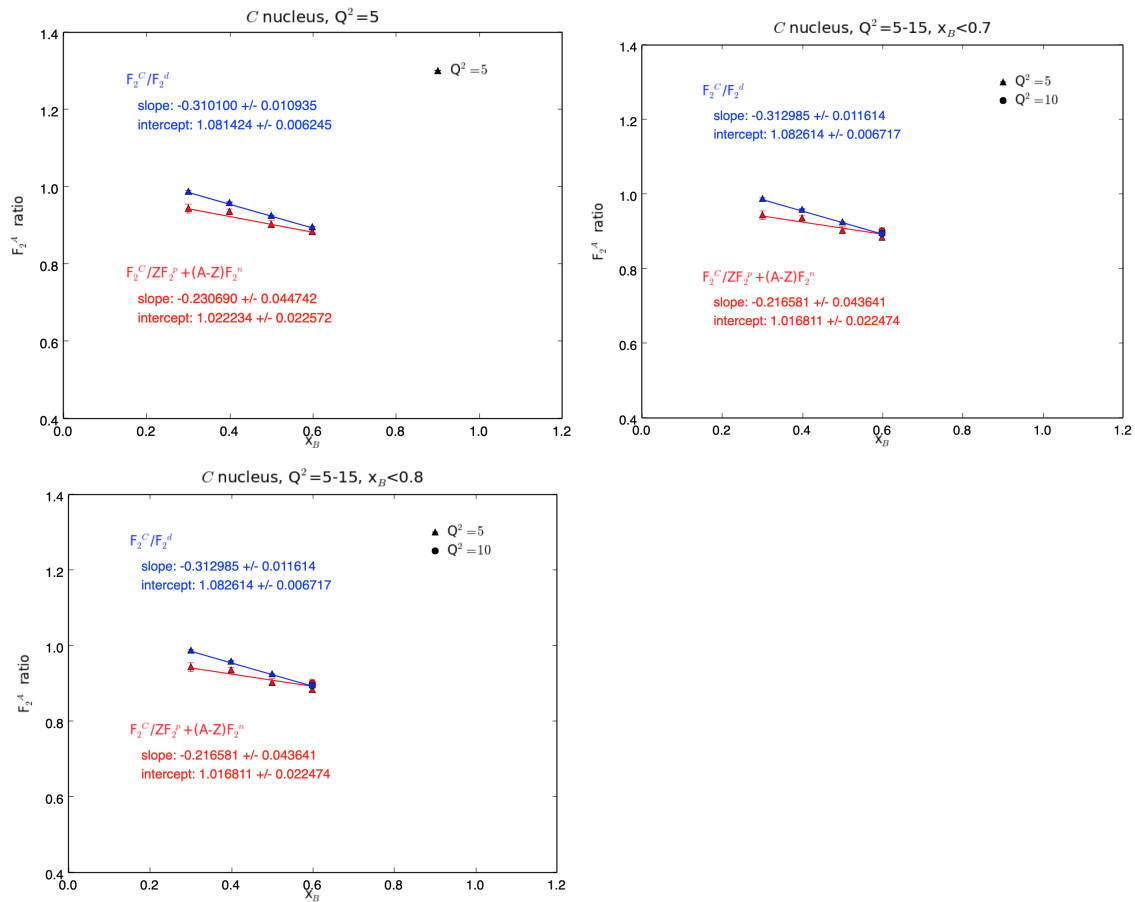


Figure 11: Linear fits to the C target data with cuts on Q^2 and x_B .

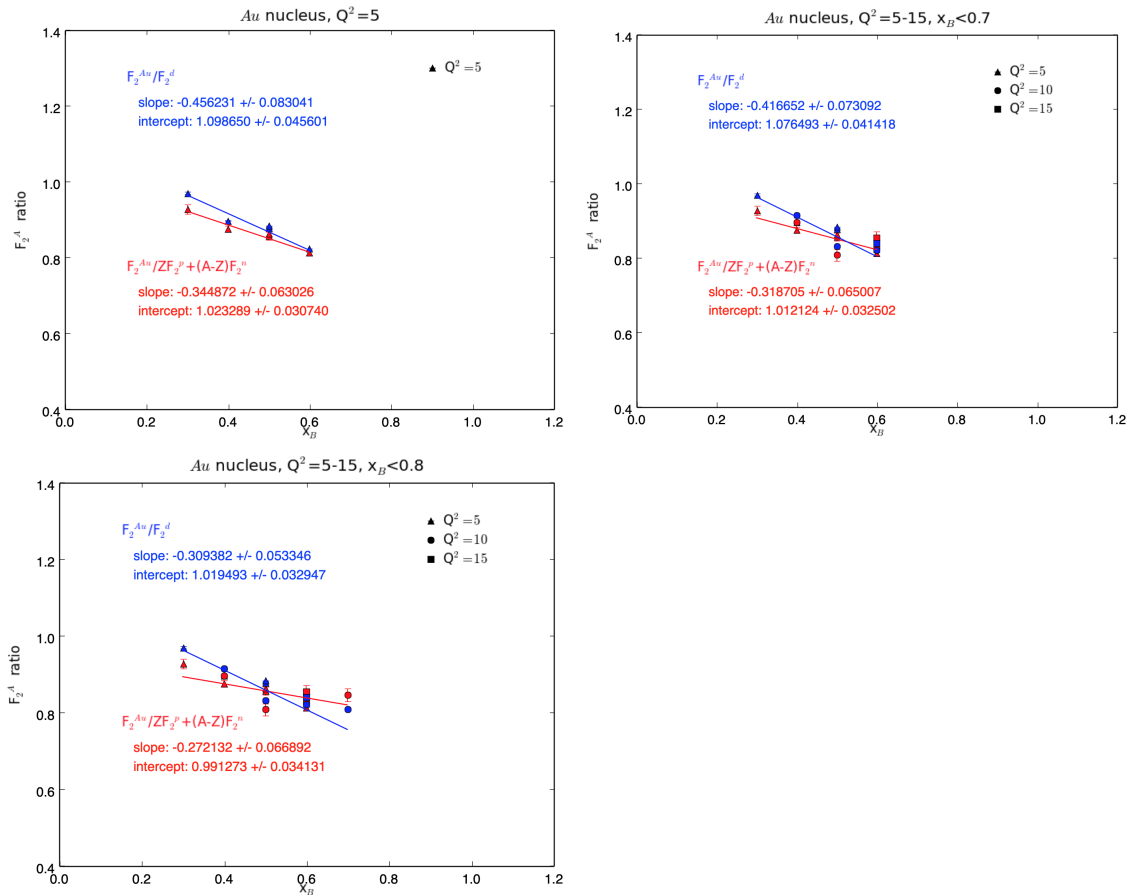


Figure 12: Linear fits to the Au target data with cuts on Q^2 and x_B .

Table 1: Summary of linear fits to x_B where $Q^2 = 5$.

Nucleus	A/d slope	A/d intercept	A/(n+p) slope	A/(n+p) intercept
deuterium	0.034078 +/- 0.013514	0.963954 +/- 0.007694	0.131192 +/- 0.028952	0.893476 +/- 0.013877
He4	-0.139559 +/- 0.041514	1.010444 +/- 0.023729	-0.054561 +/- 0.053741	0.947196 +/- 0.027083
Be	-0.153575 +/- 0.004225	1.020754 +/- 0.002375	-0.064459 +/- 0.041653	0.955925 +/- 0.020121
C	-0.310100 +/- 0.010935	1.081424 +/- 0.006245	-0.230690 +/- 0.044742	1.022234 +/- 0.022572
Al	-0.308688 +/- 0.058075	1.074479 +/- 0.032618	-0.241920 +/- 0.085474	1.021834 +/- 0.042052
Ca	-0.327402 +/- 0.048885	1.085172 +/- 0.027035	-0.27227 +/- 0.051774	1.037505 +/- 0.025103
Fe	-0.368335 +/- 0.041561	1.085849 +/- 0.022646	-0.286425 +/- 0.062250	1.024809 +/- 0.029771
Ag	-0.423013 +/- 0.087616	1.119710 +/- 0.048607	-0.360732 +/- 0.113255	1.068858 +/- 0.055132
Au	-0.456231 +/- 0.083041	1.098650 +/- 0.045601	-0.344872 +/- 0.063026	1.023289 +/- 0.030740

Table 2: Summary of linear fits to x_B where $Q^2 = 5 - 15$ and $x_B < 0.7$.

Nucleus	A/d slope	A/d intercept	A/(n+p) slope	A/(n+p) intercept
deuterium	0.021260 +/- 0.020875	0.974781 +/- 0.011910	0.150795 +/- 0.039755	0.894508 +/- 0.019402
He4	-0.118090 +/- 0.035769	0.997067 +/- 0.020596	-0.016222 +/- 0.045129	0.931353 +/- 0.023103
Be	-0.197454 +/- 0.083778	1.035493 +/- 0.048067	-0.059106 +/- 0.030303	0.953386 +/- 0.015144
C	-0.312985 +/- 0.011614	1.082614 +/- 0.006717	-0.216581 +/- 0.043641	1.016811 +/- 0.022474
Al	-0.298244 +/- 0.057500	1.070859 +/- 0.032829	-0.210889 +/- 0.056564	1.010775 +/- 0.028368
Ca	-0.334267 +/- 0.034303	1.088128 +/- 0.019560	-0.247045 +/- 0.051788	1.027656 +/- 0.025990
Fe	-0.379082 +/- 0.040058	1.085956 +/- 0.022621	-0.257315 +/- 0.043599	1.010276 +/- 0.021402
Ag	-0.432939 +/- 0.060259	1.124006 +/- 0.034442	-0.338549 +/- 0.081071	1.060178 +/- 0.040839
Au	-0.416652 +/- 0.073092	1.076493 +/- 0.041418	-0.318705 +/- 0.065007	1.012124 +/- 0.032502

[3] K. A. Griffioen *et al.*, “Measurement of the EMC Effect in the Deuteron,” Phys. Rev. C **92**, no.

Table 3: Summary of linear fits to x_B where $Q^2 = 5 - 15$ and $x_B < 0.8$.

Nucleus	A/d slope	A/d intercept	A/(n+p) slope	A/(n+p) intercept
deuterium	-0.047904+/-0.020441	1.011339+/-0.013123	0.173649+/-0.034450	0.885021+/-0.017643
He4	-0.066610+/-0.025529	0.969128+/-0.015975	0.024671+/-0.050676	0.913125+/-0.026599
Be	-0.105347+/-0.056027	0.986067+/-0.035211	-0.016830+/-0.042937	0.934997+/-0.022080
C	—	—	—	—
Al	-0.268256+/-0.036285	1.054884+/-0.022384	-0.178675+/-0.057032	0.996550+/-0.029163
Ca	—	—	—	—
Fe	-0.265522+/-0.041894	1.026296+/-0.025600	-0.219929+/-0.048613	0.994104+/-0.024310
Ag	—	—	—	—
Au	-0.309382+/-0.053346	1.019493+/-0.032947	-0.272132+/-0.066892	0.991273+/-0.034131

1, 015211 (2015) doi:10.1103/PhysRevC.92.015211 [arXiv:1506.00871 [hep-ph]].

- [4] J. G. Rubin, J. Arrington, “A New Extraction of Neutron Structure Functions from Existing Inclusive DIS Data,” doi: 10.1063/1.3631528 [arXiv:1101.3506v2 [nucl-ex]].
- [5] L.W.Whitlow, SLAC-Report-357, Ph.D. Thesis, Stanford University, March 1990.
- [6] <https://www.slac.stanford.edu/exp/e139/E139.RESULTS>
- [7] http://www.slac.stanford.edu/exp/e140/SIGMA.D2_357
- [8] Alekhin, S. I. and Kulagin, S. A. and Pettit, R., “Nuclear effects in the deuteron and constraints on the d/u ratio,” Phys. Rev. D **96**, no. 5, 0054005 (2017) doi:10.1103/PhysRevD.96.054005 [arXiv:1704.00204].
- [9] S. Malace, D. Gaskell, D. W. Higinbotham and I. Cloet, “The Challenge of the EMC Effect: existing data and future directions,” Int. J. Mod. Phys. E **23**, no. 08, 1430013 (2014) doi:10.1142/S0218301314300136 [arXiv:1405.1270 [nucl-ex]].

9 Appendix

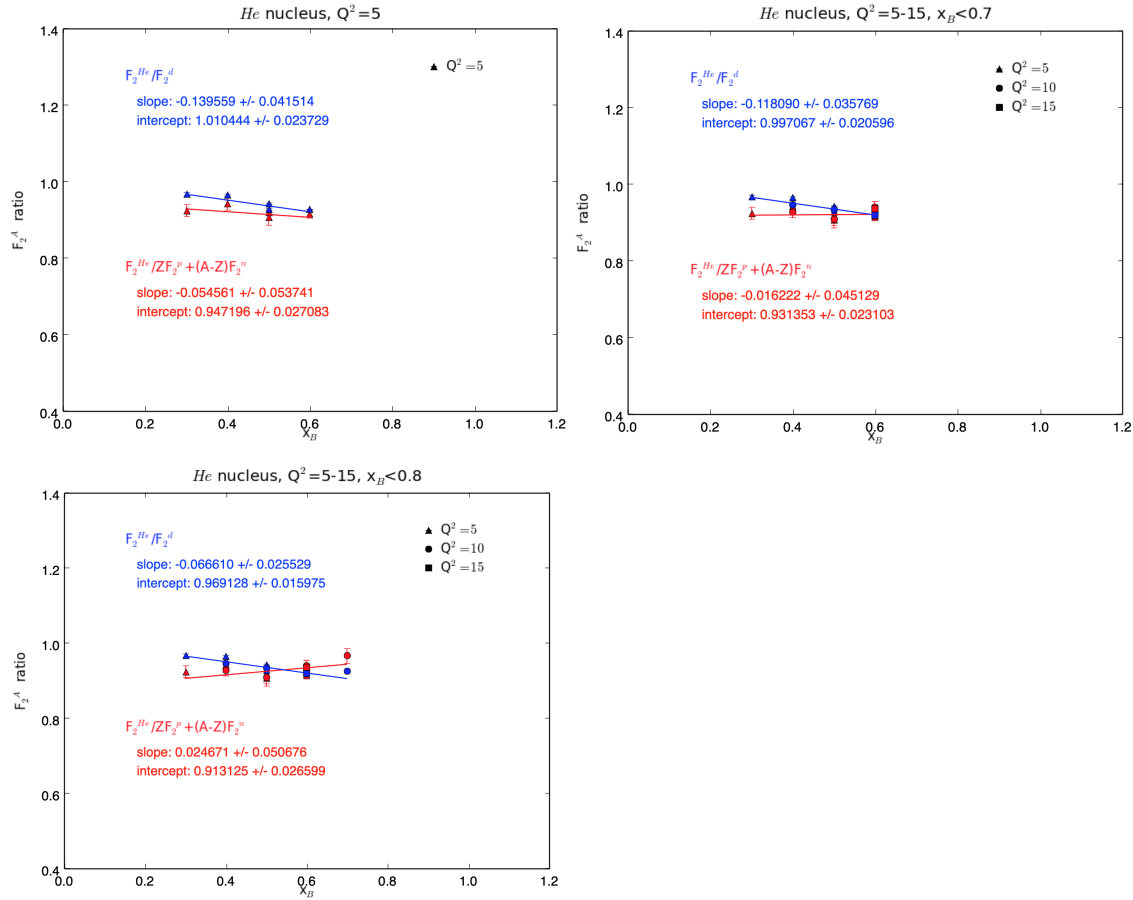


Figure 13: Linear fits to the He target data with cuts on Q^2 and x_B .

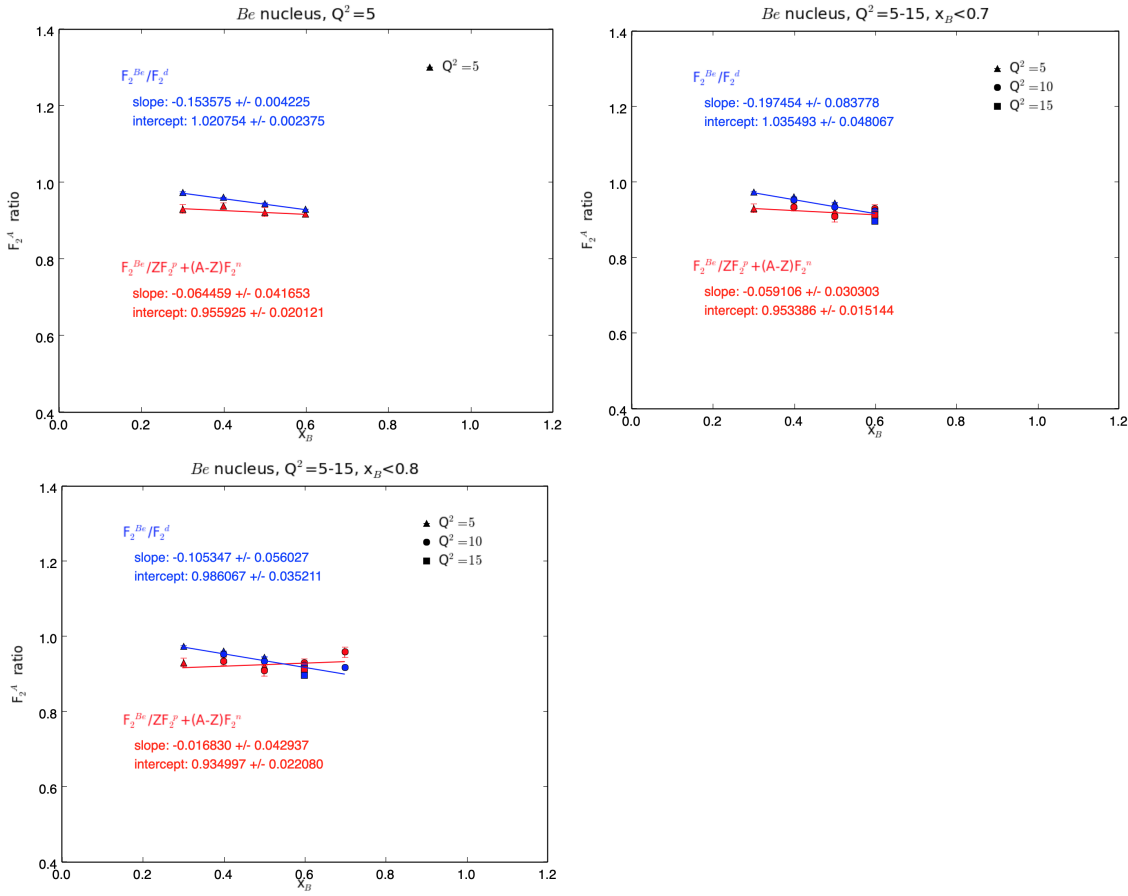


Figure 14: Linear fits to the Be target data with cuts on Q^2 and x_B .

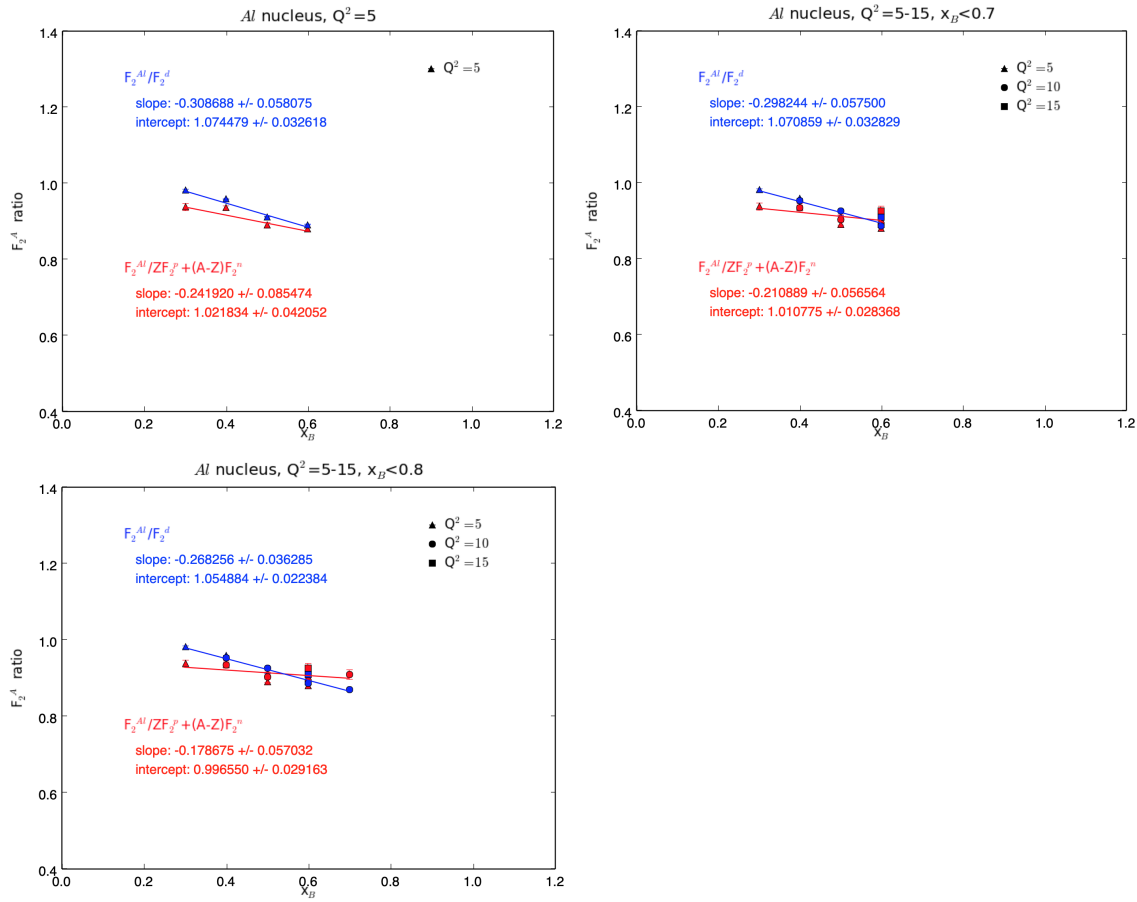


Figure 15: Linear fits to the Al target data with cuts on Q^2 and x_B .

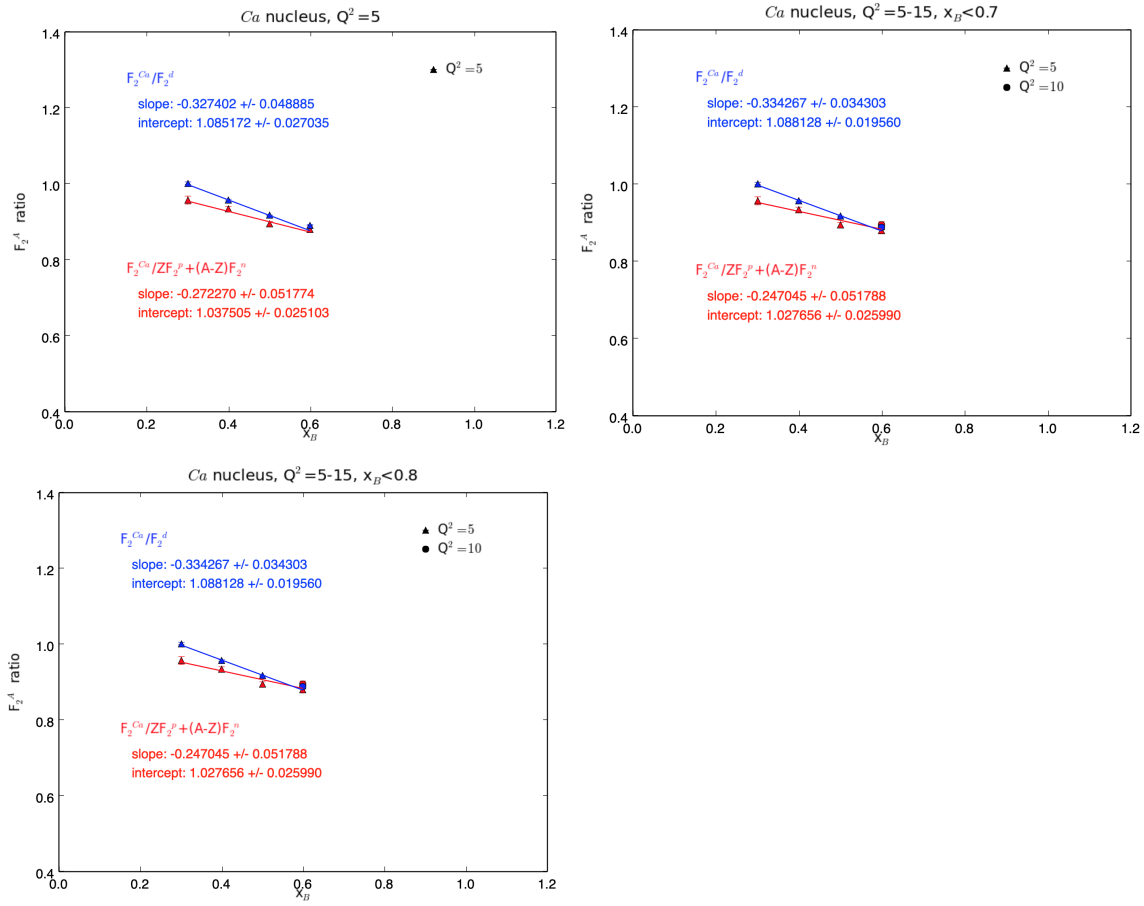


Figure 16: Linear fits to the Ca target data with cuts on Q^2 and x_B .

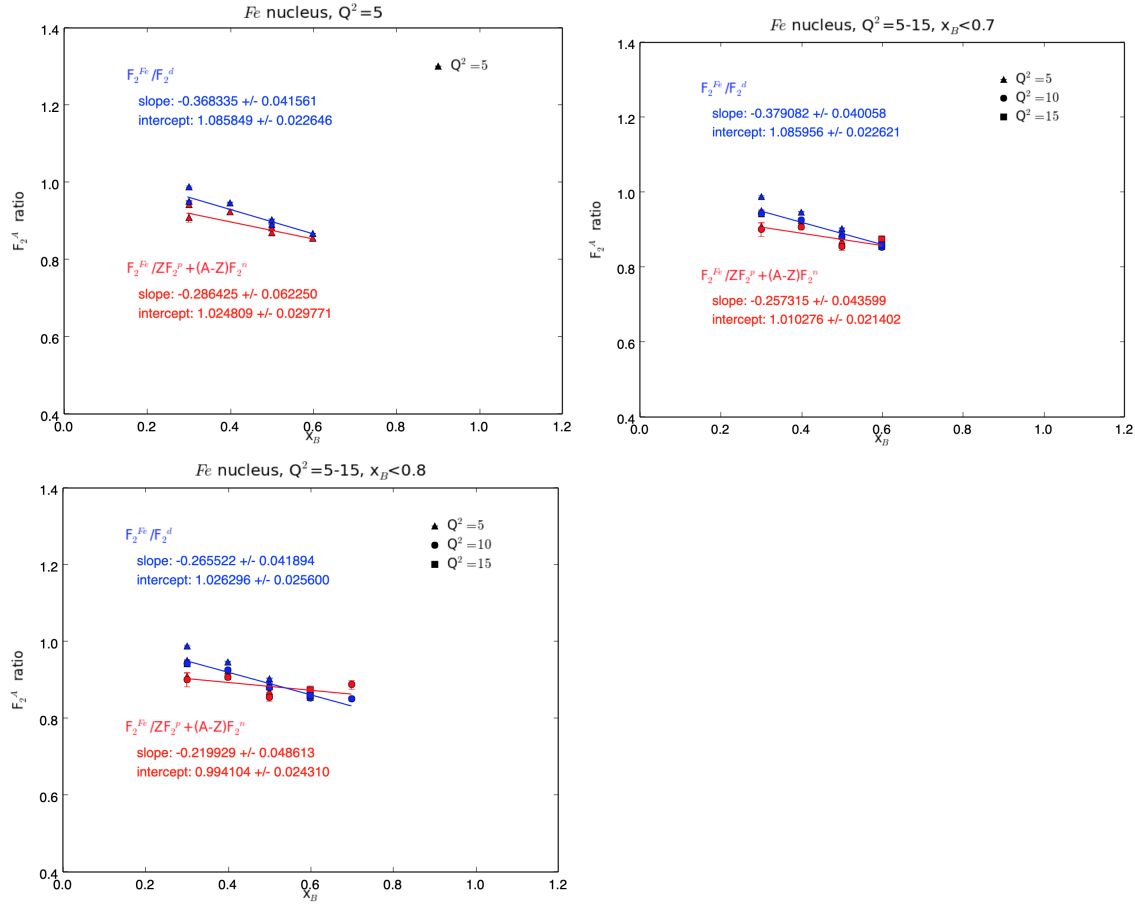


Figure 17: Linear fits to the Fe target data with cuts on Q^2 and x_B .

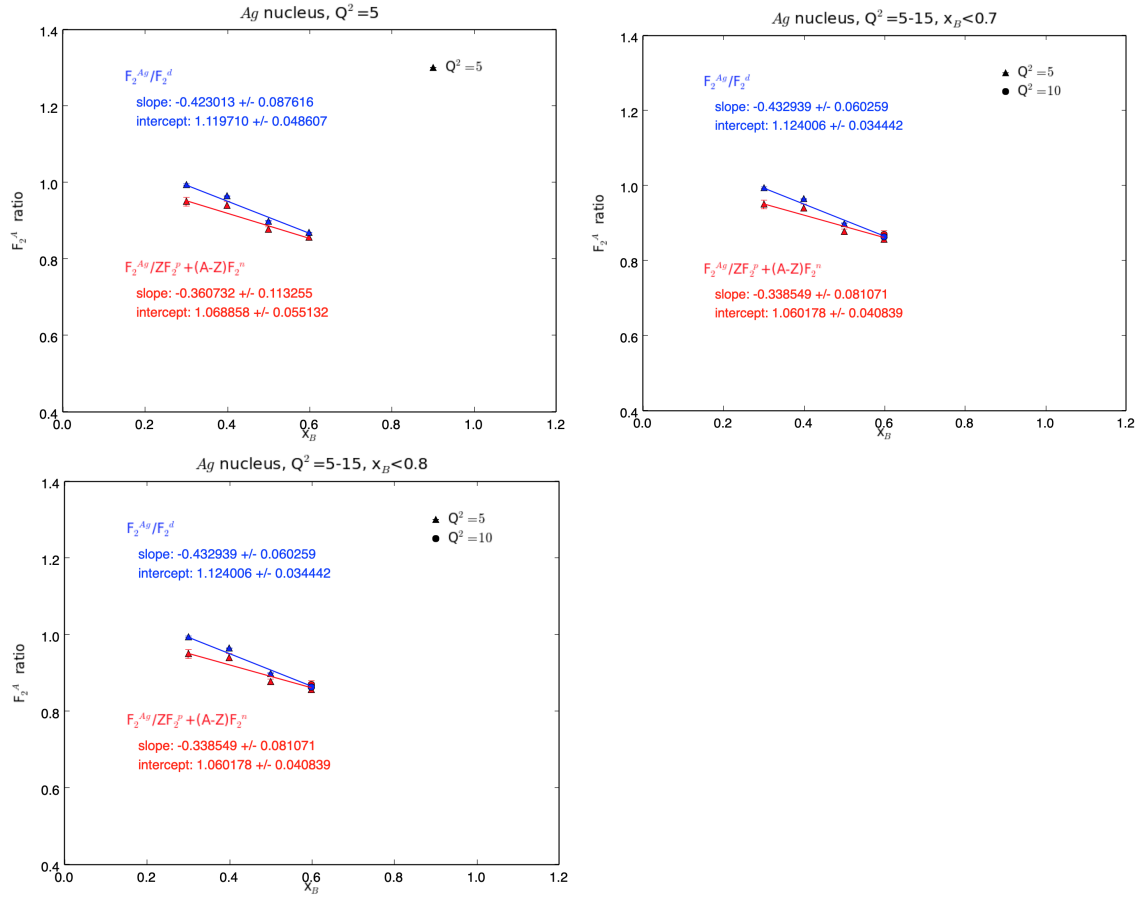


Figure 18: Linear fits to the Ag target data with cuts on Q^2 and x_B .

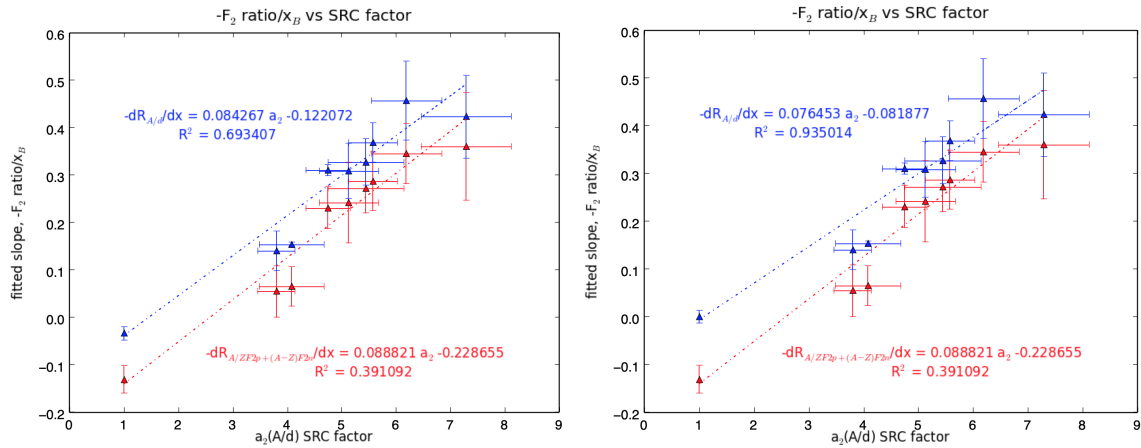


Figure 19

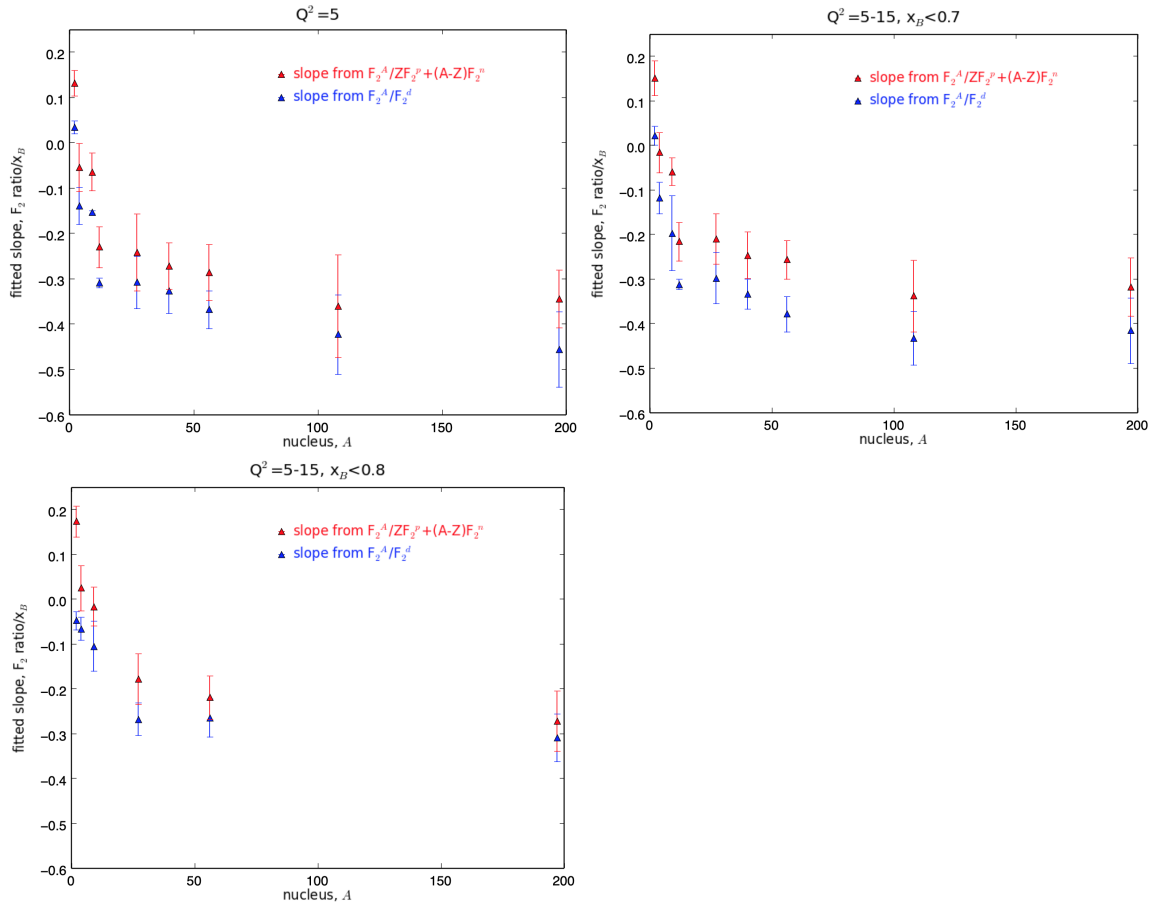


Figure 20: .

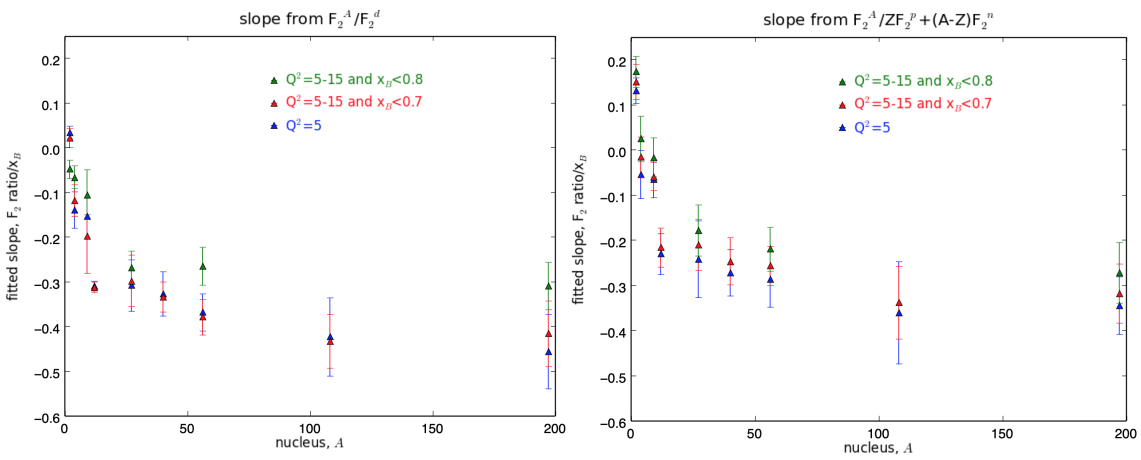


Figure 21: .